

Received October 4, 2015, accepted October 15, 2015, date of publication November 5, 2015, date of current version November 16, 2015.

Digital Object Identifier 10.1109/ACCESS.2015.2498105

Revenue Optimization Frameworks for Multi-Class PEV Charging Stations

CUIYU KONG¹, (Student Member, IEEE), ISLAM SAFAK BAYRAM^{2,3}, (Member, IEEE), AND MICHAEL DEVETSIKIOTIS¹, (Fellow, IEEE)

¹Department of Electrical and Computer Engineering, North Carolina State University, Raleigh, NC 27695-7911, USA

²College of Science and Engineering, Hamad Bin Khalifa University, Doha, 5825, Qatar

³College of Science and Technology, Hamad Bin Khalifa University, Doha 5825, Qatar

Corresponding author: C. Kong (ckong3@ncsu.edu)

ABSTRACT The charging power of plug-in electric vehicles (PEVs) decreases significantly when the state of charge (SoC) gets closer to the fully charged state, which leads to a longer charging duration. Each time when the battery is charged at high rates, it incurs a significant degradation cost that shortens the battery life. Furthermore, the differences between demand preferences, battery types, and charging technologies make the operation of the charging stations a complex problem. Even though some of these issues have been addressed in the literature, the charging station modeling with battery models and different customer preferences have been neglected. To that end, this paper proposes two queueing-based optimization frameworks. In the first one, the goal is to maximize the system revenue for single class customers by limiting the requested SoC targets. The PEV cost function is composed of battery degradation cost, the waiting cost in the queue, and the admission fee. Under this framework, the charging station is modeled as a $M/G/S/K$ queue, and the system performance is assessed based on the numerical and simulation results. In the second framework, we describe an optimal revenue model for multi-class PEVs, building upon the approach utilized in the first framework. Two charging strategies are proposed: 1) a dedicated charger model and 2) a shared charger model for the multi-class PEVs. We evaluate and compare these strategies. Results show that the proposed frameworks improve both the station performance and quality of service provided to customers. The results show that the system revenue is more than doubled when compared with the baseline scenario which includes no limitations on the requested SoC.

INDEX TERMS Electric vehicle, queuing system, multi-class, dedicated chargers, shared chargers.

NOMENCLATURE

R	Reward after completing the service of a PEV
SoC_i	Initial SoC of a PEV
SoC_r	Requested SoC of a PEV
C_{total}	Total cost for a PEV
p	Admission fee of a PEV
R_e	System revenue
P_K	Blocking probability when number of customers is K
E_c	The threshold energy
E_i	Initial energy of a PEV
E_r	Requested energy of a PEV
P_{max}	Maximum charging power for a PEV
J	Number of distinct PEV classes
λ_j	Arrival rate of class j
s_j	Number of chargers allocated to class j
θ_j	Proportion of total arrival rate of system λ for type j

$R_{e,d}^j$	Class revenue of class j in dedicated charger model
$R_{e,s}^j$	Class revenue of class j in shared charger model
CCCV	Constant current constant voltage.

I. INTRODUCTION

A. BACKGROUND AND MOTIVATION

Plug-in electric vehicles (PEVs) are gradually gaining mainstream acceptance, as they provide a great potential for reducing the carbon footprint. PEVs also offer savings in fuel and maintenance costs over gas-powered counterparts, as the cost of electricity is lower and the electric motors are more stable [1]. Therefore, there has been an impetus towards the PEVs and more than 800 000 vehicles have been sold worldwide since late 2010. This trend is further supported by the policy-makers and expected to grow well into the next decades, as electrifying transportation systems

strengthens energy security and independence since electricity can be generated through a diverse set of domestic sources [2], [3]. For instance, in Norway PEV sales have already reached 22% of the new vehicle sales in the first quarter of 2015.

The performance of a PEV is related with the underlying battery technology. For example specific energy (Wh/kg) and energy density (Wh/Liter) characteristics of the battery determines the additional weight and the space required to install the onboard battery, which also determines the all-electric driving range. Another important battery characteristics are the cycle and calendar life which are primarily affected by the charging/discharging power of the battery. The U.S. Advanced Battery Consortium is aiming to develop storage technologies that could last for 15 years under the slow charging scenario. On the other hand, Level 1 slow charging stations may not be accessible or desirable for many users. For instance, in densely populated countries, e.g., Japan, Netherlands, and Norway, fast public stations are more convenient to extend the all-electric range in a short amount of time.

In such facilities, two types of problems arise. The first problem is that the uncontrolled and concurrent charging of PEVs could have disruptive effects on the power grid such as transformer and line overloading, power quality deterioration, and supply-demand imbalances [4]–[6]. The second issue, on the other hand, is that high charging power can degrade the battery health, and hence diminish the cost-effectiveness of PEVs. To that end, this paper presents an optimization framework that addresses the battery health and charging duration trade-off.

B. RELATED WORKS

We continue to present the related literature for the two issues mentioned above. For the first problem, there has been a growing body of literature on control, scheduling, and optimization for PEV charging stations to alleviate the adverse impacts of PEV load. Overall, the related studies can be divided into two categories: load control at a single charging station and load management at a network of charging stations. Moreover, each group may assume single or multiple classes of customers that are typically grouped according to the charging rate. For instance, the works presented in [7]–[11] proposed queueing-based single charging station models and pricing-based admission control frameworks to control the aggregated demand within the grid operating limits. Another approach to alleviate the stochastic demand is to employ energy storage units which act as energy buffers to smooth the spikes [7], [8].

In the multiple station setting, the idea is to route customers to neighboring stations, so that customers can receive service with a certain level of quality of service (QoS), that is typically the waiting time or the blocking (loss-of-load) probability. The work in [12] proposed a centralized control framework and assigns customers to idle stations, while the works in [14] and [15] presented decentralized

control structures to reduce the load among the stations. From the modeling standpoint, authors in [16] proposed a spatial and temporal model in dynamic PEV traffic system by adopting $M/M/s$ queues to formulate the charging demand. In [17], the authors considered the demand response at multiple charging stations, and modeled each charging station as $M/M/1$ queuing system. Aiming to minimize the waiting time for PEVs, authors in [17] formulated the optimization problem and provided an optimal PEV allocation algorithm and pricing mechanism to achieve the goal.

Recently, battery degradation cost has received some attention in the literature, as high charging rates shortens the battery health. In [18], authors proposed a method to minimize the cost of PEVs including the battery degradation cost., while the study presented in [19] showed a distributed method to coordinate the charging strategies of PEVs with battery degradation cost. [18], [19] considered a model with the battery degradation cost defined from the perspective of power engineering.

Due to their high energy density and low self-discharge, characteristics Lithium-ion (Li-ion) batteries are widely preferred in PEVs. For such battery technologies, DC fast charging uses constant current constant voltage (CCCV) method, which works as follows [9] and [20]. The charging current remains constant when current is less than a threshold value. When the current reaches the threshold, the voltage is kept constant, but due to the internal resistance of the battery, the charging current drops exponentially. Therefore, it takes a longer time to charge higher SoC levels, e.g., from 90% to 95%, than charging the same amount of energy in the lower levels, e.g., from 30% to 35% [9]. The investigation of this behavior is critical in charging station designs and load control frameworks.

This study also complements our previous works: in [8], [12], and [13], we present a queueing-based fast charging station model equipped with energy storage devices, whereas the works presented in [7] and [15] provide mathematical frameworks for load balancing in a fast charging network. However, in this paper we provide a more holistic approach and take the electrochemical properties of the battery technology in the account.

C. CONTRIBUTIONS

In this paper, we consider a small-scale fast public charging station and propose optimization frameworks to maximize the station revenue. The proposed frameworks contribute to the existing literature in the following ways.

- We model the charging facility as a $M/G/S/K$ queue and choose the blocking probability and waiting time as the QoS metrics. We analyze the queueing model and support the numerical results with simulation studies. Furthermore, we present a detailed battery cost model for Li-ion batteries, which are widely used for automotive applications.

- We propose two different optimization frameworks. In the first one, single-class customers are considered and an optimal revenue model is proposed. In the model, customers gain reward by reaching higher SoC levels, while the cost of battery degradation, customer discomfort due to waiting and blocking events, and admission fee constitute the cost part.
- We extended our work to a multi-class setting, where customers are differentiated by their preferences; sizes of their battery packs, amounts of requested demands, and the available charger technologies. In addition to the aforementioned revenue model, we propose two charging strategies: shared chargers and dedicated chargers for different classes. We show that under different traffic regimes, the operating revenue can be increased by optimally choosing the charging strategy.

The remainder of this paper is organized as follows: Section II presents the optimal system revenue framework for single class PEVs, including the battery degradation cost, formulation of an admission fee, system revenue model, charging power model and *M/G/S/K* queuing model. Section III discusses and analyzes the numerical and simulation results for the performance. In Section IV, an optimal system revenue framework for multi-class PEVs is proposed. First, the dedicated chargers model is analyzed and numerical and simulation results are presented. Next, the shared chargers model is studied, and the simulation results are compared with the case of dedicated chargers. From the simulation results, it is shown that the decision for the appropriate charging strategy is primarily governed by the traffic intensity.

II. OPTIMAL SYSTEM REVENUE FRAMEWORK FOR SINGLE-CLASS CUSTOMERS

In this section, we present the optimization framework for the single-class case. The main goal of the proposed framework is to limit the state of charge demand of vehicles at a reasonable level, e.g., 90% SoC, so that the station revenue is maximized by serving more vehicles. The rationale behind this is that charging power duration increases as the battery SoC is getting closer to the full state. Therefore, the core of the framework is the battery charging model and the battery degradation cost which is related to the conventional constant current constant voltage method of the Li-ion batteries. Furthermore, the system revenue depends on the stochastics involved with the customer demand such as mean waiting time and the blocking probability, therefore a queueing analysis is also provided.

A. CHARGING POWER MODEL

CCCV method is widely used for Li-ion battery charging, as it protects the battery life. During the charging, the current remains constant until it reaches the threshold value. After the threshold, the voltage (V) is maintained at a fixed value and the charging current (A) decreases exponentially. In terms of charging power (kW), from the empty battery to a threshold energy, the charging power remains constant. Once the energy

reaches the threshold, the charging power is decreasing with the increment of SoC. In this study, the charging power function in [9] is adopted, which is:

$$P(E) = \begin{cases} P_{\max} & E < E_c \\ m_1 - n_1 \cdot E & \text{otherwise,} \end{cases} \quad (1)$$

where E is the energy in the battery and E_c is the threshold energy for the mode from constant power to the decreasing power. m_1 and n_1 are the constant parameters in [9], and P_{\max} is the maximum charging power for a PEV, as shown in Fig. 1.

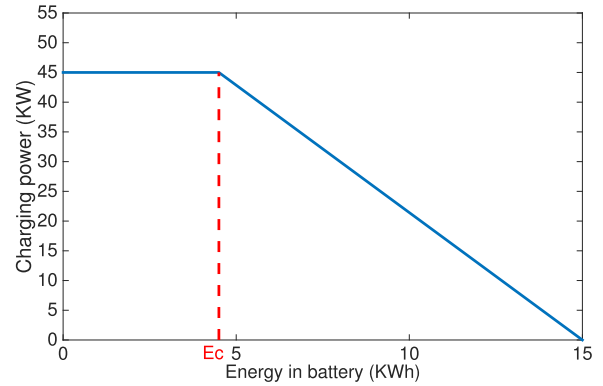


FIGURE 1. Charging power function [9].

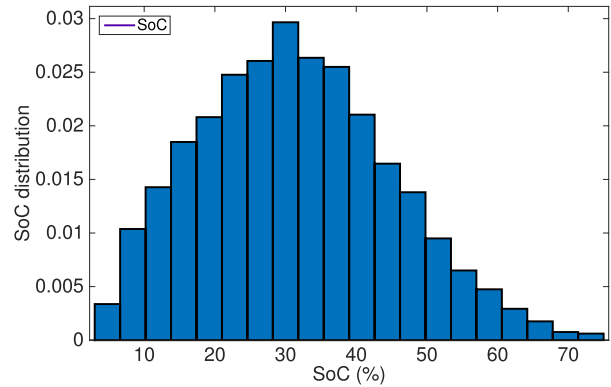


FIGURE 2. Initial SoC distribution of arriving PEVs.

The charging times are related to the initial (E_i) and requested SoC (E_r) levels and the charging power. We assume the SoC distribution is obtained via historical data and known by the station operator. Then, for a given SoC distribution, an example presented in Fig. 2, the charging duration distribution can be obtained by the following,

$$t = \begin{cases} \frac{E_c - E_i}{P_{\max}} + \frac{1}{n_1} \log \left(\frac{m_1 - n_1 \cdot E_c}{m_1 - n_1 \cdot E_r} \right), & E_i \leq E_c \\ \frac{1}{n_1} \log \left(\frac{m_1 - n_1 \cdot E_i}{m_1 - n_1 \cdot E_r} \right), & E_i > E_c \end{cases} \quad (2)$$

Notice that the first component represents the time it takes to charge the vehicle, which is the amount of energy transfer from the initial SoC to the threshold value divided by the constant charging power. While the natural logarithmic

component represents the energy transfer after the threshold value. Of note, the SoC is assumed to be bounded between 0 – 100%.

As given in [9], [21], and [22], the initial state of charge SoC_i distribution follows a normal distribution and it is set to be $\mathcal{N}(30, 15)$, where the mean is 30 and standard variation is 15. And it is truncated to target SoC internal of $[5, SoC_r - 10]\%$. The example illustrated in Fig.2 shows the distribution of SoC_i when SoC_r is set to 85%. Thus, knowing the distribution of SoC_i and (2), the distribution of charging times can be obtained. For the given settings, the results are shown in Fig.3.

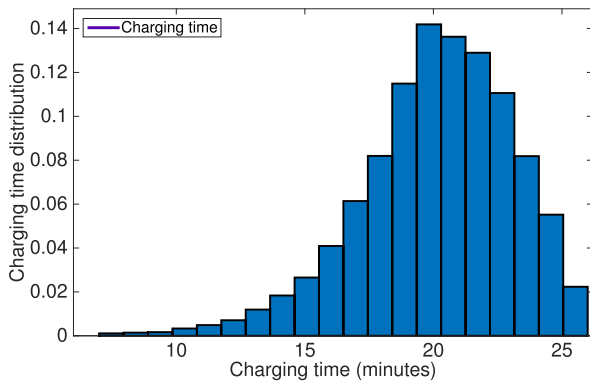


FIGURE 3. Charging time distribution $SoC_r = 85\%$.

Moreover, from the charging time distribution, the mean charging time $\mathbb{E}(t_{ch})$ is known. Then the mean charging power $\mathbb{E}(P_{ow})$ can be obtained as

$$\mathbb{E}(P_{ow}) = \frac{E_r - \mathbb{E}(E_i)}{\mathbb{E}(t_{ch})}, \quad (3)$$

where $\mathbb{E}(E_i)$ is the mean value for E_i . It is noteworthy that the charging time and the charging power are a function of the requested state of charge level SoC_r . For higher SoC_r , the required charging time increases and the charging power decreases.

B. BATTERY DEGRADATION COST

As the vast majority of car manufacturers employ Li-ion batteries, we choose to analyze them in our battery model. Each time the battery is charged, there is an associated degradation cost, which is a function of the charging power and the charging duration [19]. The battery degradation becomes a critical element under the high charging regime, as it shortens the life cycle of the battery. Therefore, we include battery degradation cost in our optimization framework as a function of the charging power and the battery characteristics [19]. The expected battery degradation cost can be represented by,

$$\mathbb{E}(c_{batt}) = a \cdot (\mathbb{E}(P_{ow}))^2 + b \cdot \mathbb{E}(P_{ow}) + c, \quad (4)$$

where P_{ow} is the mean charging power of a PEV. The remaining parameters represent a typical Li-ion battery characteristics and selected as $a = (10^6/M) \cdot V_{norm} \cdot \Delta T \cdot Pr_{cell} \cdot \alpha$,

$b = 10^3 \cdot V_{norm} \cdot \Delta T \cdot Pr_{cell} \cdot \beta$ and $c = M \cdot V_{norm} \cdot \Delta T \cdot Pr_{cell} \cdot \gamma$ [19]. Here M , V_{norm} , ΔT and Pr_{cell} are denoted as the number of cell units in a PEV, open circuit voltage of a Li-ion cell unit, the length of charging interval t , and price of single energy unit in a battery cell. α , β , and γ are defined in [19], which are functions of V_{norm} . Once the battery type of an PEV is known, the values of a , b and c can be calculated. Thus from mean charging power $\mathbb{E}(P_{ow})$ during mean charging time $\mathbb{E}(t_{ch})$, the cost of a PEV incurs is $\mathbb{E}(c_{batt}) \cdot \mathbb{E}(t_{ch})$.

C. ADMISSION FEE

A customer who joins the system gains reward R after completing the service. When the SoC_r is higher, PEV is more satisfied, and earns a higher reward. We adopt a linear reward function, that is

$$R = m \cdot SoC_r + n, \quad (5)$$

where m and n are the constant positive parameters. A PEV pays the admission fee p to join the system. On the other hand, there is a waiting cost due to delayed service, and a battery degradation cost upon charging the battery. Therefore, the total cost for a PEV is

$$C_{total} = p + c_w \cdot \mathbb{E}(t_w) + \mathbb{E}(c_{batt}) \cdot \mathbb{E}(t_{ch}), \quad (6)$$

where c_w is a constant representing the waiting cost per time unit and $\mathbb{E}(t_w)$ is the mean waiting time of a PEV in the queue.

The system owner can increase the admission fee to get more system profit [23], while the users accept to join the system only if the reward R is larger than the total cost C_{total} , that is $R \geq p + c_w \cdot \mathbb{E}(t_w) + \mathbb{E}(c_{batt}) \cdot \mathbb{E}(t_{ch})$. In other words, the reward should be equal or larger than the cost of an admission fee, waiting cost, and battery degradation cost. Hence, the maximum admission fee paid by a PEV can be calculated by

$$p = R - c_w \cdot \mathbb{E}(t_w) - \mathbb{E}(c_{batt}) \cdot \mathbb{E}(t_{ch}). \quad (7)$$

The revenue of system operator is composed by the admission fee paid by PEVs and the number of arrivals in each time unit. Thus, it's necessary to know the arrival rate of PEVs. The following subsection presents the system revenue model.

D. SYSTEM REVENUE MODEL

In the $M/G/S/K$ queue system, there are S chargers and r waiting spaces, where $r = K - S$. The PEVs arrive according to the exponential distribution with arrival rate λ . The charging time follows a general distribution, which is a function of SoC_r and charging power P_{ow} . Notice that, due to limited service space, if there are K customers in the system, the new arrivals will not be able to join the system, hence will be blocked. Let P_K denote the blocking probability of the system for a given arrival rates, customer demand, and charge rates. Then the system revenue R_e can be calculated by

$$R_e = \lambda \cdot (1 - P_K) \cdot p. \quad (8)$$

Substituting p in (7), we get

$$R_e = \lambda \cdot (1 - P_K) \cdot (R - c_w \cdot \mathbb{E}(t_w) - \mathbb{E}(c_{batt}) \cdot \mathbb{E}(t_{ch})). \quad (9)$$

In the above equation, P_K , R , $\mathbb{E}(t_w)$, $\mathbb{E}(c_{batt})$ and $\mathbb{E}(t_{ch})$ are functions of SoC_r . When SoC_r is higher, on one hand, the reward for customers R is higher. On the other hand, this translates into higher mean charging time $\mathbb{E}(t_{ch})$, which leads to higher blocking rate, higher mean waiting time, and less revenue for the station. Hence, the proposed method aims to determine the optimal SoC_r to gain the optimal system revenue. In the following subsection, relationships between charging power, charging time and SoC_r are illustrated.

E. M/G/S/K QUEUING MODEL IN CHARGING SYSTEM

We start our analysis by deriving an expression for the blocking probability P_K . The customers will be blocked when there are K customers in system because of the limited service space, which is given by

$$P_K = \frac{(S\rho)^S}{S!} \zeta^{K-S} P_0 \quad (10)$$

The procedures to find P_K , ζ and P_0 are given in Appendix A. Once we know the arrival rate λ , the number of servers S , and the mean service rate $\mu = 1/\mathbb{E}(t_{ch})$, the blocking probability of $M/G/S/K$ can be approximated. Notice that the blocking probability is also a function of SoC_r , since service rate μ is determined by the target state of charge level. For the better evaluation of system performance, the approximation of mean waiting time is derived, which is also given in Appendix A.

F. PERFORMANCE ANALYSIS IN SINGLE CLASS CUSTOMERS

In this subsection, a case study for a DC fast charging station is presented to determine the optimal SoC_r for the optimal system revenue. The proposed method is compared to the case when SoC_r is not limited, which serves as a baseline scenario.

From the relation between charging power and SoC_r , if the battery is charged to be 100% SoC_r , the charging time will be large when compared to lower SoC_r targets. Hence, the proposed method aims to limit the demand of PEVs, which is SoC_r , to maximize system revenue in (9). The assumed range of SoC_r is between 60 to 95% in the proposed method. Starting from $SoC_r = 60\%$, each time the value is increasing by 5% until reaching 95%. After the finite iterations, the optimal system revenue among these enumerations is selected.

A Matlab script was used to model the numerical portion, while Java was used to simulate the model. The simulation model is run for 100 000 PEVs, and the system input parameters in Table 1 are given by $\lambda = 10$, $S = 7$, and $r = 3$.

TABLE 1. System input parameters.

Parameter	Value
λ	10/hour
SoC_i	$\mathcal{N}(30, 15)$, truncated to $[5, SoC_r - 10](\%)$
SoC_r	60:99(%)
s	7
r	3

In the first simulation setting, the target SoC_r is varied from 60% to 95% with an increment of 5%. The case when target SoC_r is 99% is also simulated and compared. The initial state of charge distribution SoC_i is chosen as $\mathcal{N}(30, 15)$, truncated to $[5, SoC_r - 10]\%$.

TABLE 2. Function input parameters.

Parameter	Value
P_{max}	45
m_1	67.5
n_1	4.5
a	0.004
b	0.075
c	0.003
c_w	20 (\$/hour)
m	9 (\$)
n	1 (\$)

Function input parameters are shown in Table 2. DC fast charging model is chosen for evaluation. Hence, the maximum charging power P_{max} , the battery capacity, and the threshold energy E_c are assumed to be 45 kWh, 15kWh, and 5 kWh respectively. Combined with (1), m_1 and n_1 are calculated to be 67.5 and 4.5 respectively. a , b and c values are adapted from [19] for Li-ion batteries. The waiting cost per hour c_w is assumed to be 20. When there's no waiting cost and no battery degradation cost, a PEV pays 10 units for admission fee p in simulation based on [26]. So the maximum reward R is set to be 10 units. Hence combined with (5), m and n are calculated to be 9 and 1 unit respectively.

In Fig.4a, we show the relationship between the mean charging time and the SoC levels. It can be seen that the charging duration from $SoC_i = 30\%$ to $SoC_r = 85\%$ takes about 20 minutes. However, the charging duration raises exponentially when the SoC_r is set to 95%, and it takes 14.7 more minutes to charge the next 10% SoC. In Fig.4b, the mean charging power is presented. As shown in the figure, when the SoC_r is set to higher values the mean charging power drops, due to the charging characteristics presented in Fig.1. Similarly, Fig.4c shows that the traffic intensity, ρ , increases with SoC_r , because the mean charging duration also grows as shown in Fig.4a.

Fig.4d and Fig.4e depict results for blocking probability and mean waiting time respectively. Similar to previous findings, higher SoC_r targets leads to undesired system performance, higher blocking rates and long waiting times. In Fig.4d and Fig.4e, numerical results are almost the same as the simulation results except for the case when $SoC_r = 99\%$. The reason for the difference between these two results when $SoC_r = 99\%$ is that the traffic intensity ρ goes to infinity and system becomes unstable.

One of the main findings of this section is presented in Fig.4f, which depicts the system revenue under different SoC_r . By varying the SoC_r from 60 to 99%, the station revenue is calculated. It is shown that for the given simulation parameters, setting SoC_r to 90% maximizes the system revenue, which is calculated as R_e^* is 74.8. The proposed

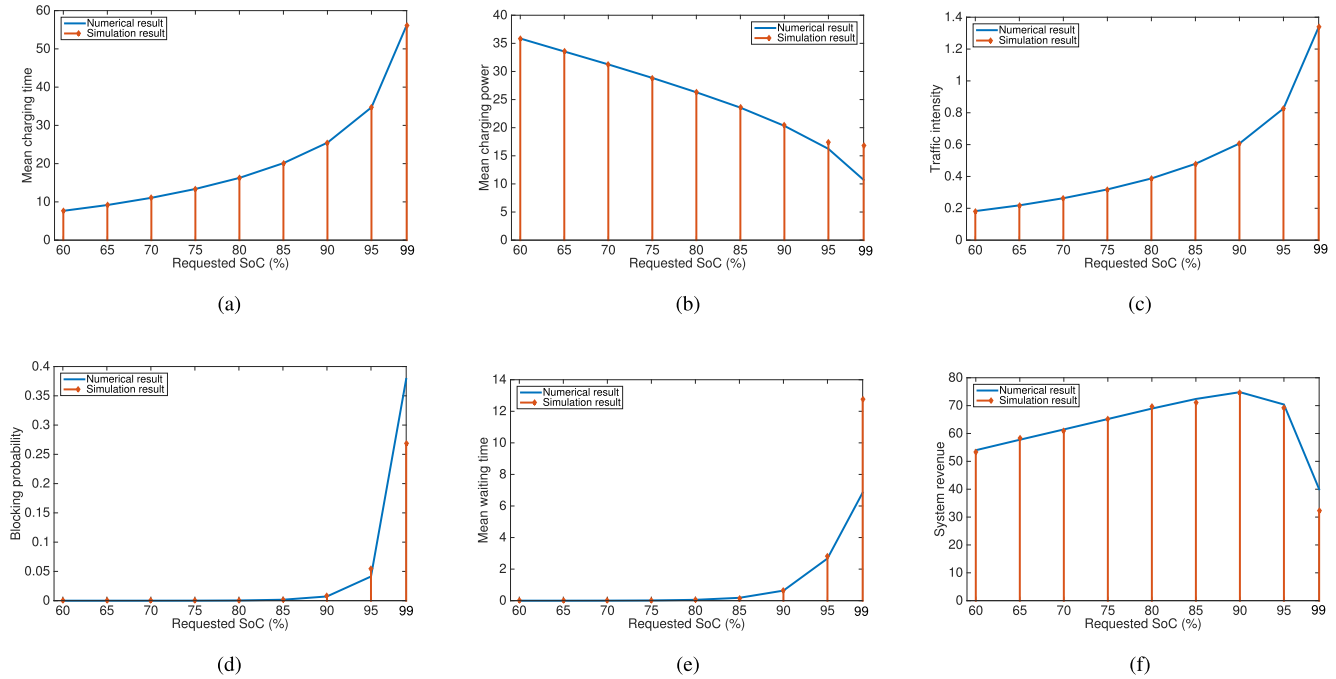


FIGURE 4. Numerical and simulation results in $M/G/S/K$ queuing system. (a) Mean charging time (minutes). (b) Mean charging power (kW). (c) Traffic intensity. (d) Blocking probability. (e) Mean waiting time (minutes). (f) System revenue/hour.

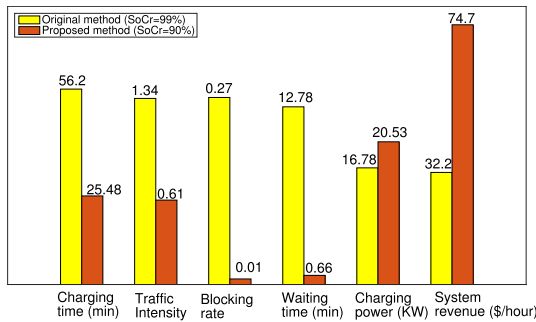


FIGURE 5. Proposed system performance comparison to original method.

framework is compared with the baseline scenario where the target SoC_r is not limited. The results presented in Fig.5 shows that the proposed method can significantly improve the system performance and more vehicles can be served with the same amount of grid resources.

III. OPTIMAL SYSTEM REVENUE FRAMEWORK FOR MULTI-CLASS CUSTOMERS

In this section, we extend the previous framework for the multi-class setting. Similar to the single-class case, the charging station is modeled with a $M/G/S/K$ queue, but this time J classes of PEVs can be served. The customer classes are differentiated by charging technology, customer preferences, and the amount of battery cell units. Therefore, the parameters in charging power function in (1) are different among different customer types $j \in \{1, 2, \dots, J\}$.

In addition to the computation of optimal SoC_r levels for each class, we propose two different resource

allocation methods. The first one is the *dedicated* charger model, in which charging resources are allocated to different customer classes. The second method, on the other hand, does not physically divide the resources and the demand is met by the *shared* resource pool. The allocation methods are depicted in Fig.6, which simply assumes that there are two classes of PEVs. The primary goal is to choose the strategy that maximizes system revenue under different traffic loads.

A. DEDICATED CHARGER MODEL

In the dedicated charger model, the primary goal is to compute the optimal composition of chargers and the SoC_r targets for each customer type. The arrival rate of type j is denoted by $\lambda_j = \theta_j \lambda$, where θ_j is the proportion of total arrival rate of system λ for type j . Similarly, the waiting space for class j is denoted by r_j . From (9), the class j revenue in dedicated chargers model is:

$$R_{e,d}^j = \theta_j \lambda \cdot (1 - P_{ro}^j) \cdot (R - c_w \cdot \mathbb{E}(t_w^j) - \mathbb{E}(c_{batt}^j) \cdot \mathbb{E}(t_{ch}^j)), \quad (11)$$

where P_{ro}^j , $\mathbb{E}(t_w^j)$, $\mathbb{E}(c_{batt}^j)$, and $\mathbb{E}(t_{ch}^j)$ are the blocking probability, the mean waiting time, the mean battery degradation cost in time unit, and the mean charging time of customer type j respectively.

The number of chargers allocated to type j is denoted by s_j . Since there a group of chargers are dedicated to each charger type the system acts as J different queues and from the analysis presented in the previous section, optimal $SoC_{r,j}^*$ for each class revenue R_e^j can be calculated.

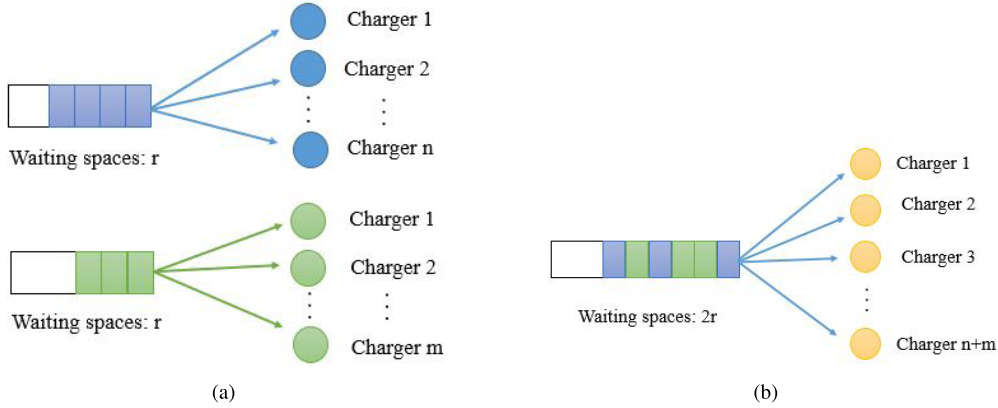


FIGURE 6. Dedicated and shared charger model. (a) Dedicated charger model. (b) Shared charger model.

Specifically, the proposed method aims to find the optimal $s_j^* \in \{1, 2, \dots, S\}$ and optimal $SoC_{r,j}^*$ to optimize the total system revenue $\sum_{j \in J} R_{e,d}^j$. Therefore, the optimal system revenue in dedicated charger method can be calculated from

$$\begin{aligned} & \arg \max \sum_{j \in J} R_{e,d}^j(\theta_j \lambda, s_j, SoC_r^j) \\ & s.t \sum_{j \in J} s_j = S \\ & \theta_j, \lambda, S, J \text{ are given} \end{aligned} \quad (12)$$

Given θ_j, λ, S and J , optimal combination of $(s_1^*, s_2^*, \dots, s_J^*)$ and optimal system revenue can be gained from the model above.

B. SHARED CHARGER MODEL

In the shared charger model, the same resource pool is shared by all customer types. The arrival rate of type j is $\lambda_j = \theta_j \lambda$, where θ_j denotes the proportion of total arrival rate of system λ for type j . The shared waiting space is denoted by r . Since all customer classes share the same chargers and waiting space, the blocking probability for each class is the same. Let P_{ro} be the blocking probability for each class in shared charger model, $P_{ro} = P_{ro}^1 = P_{ro}^2 = \dots = P_{ro}^J$. And the mean waiting time for each class is also the same because of shared waiting spaces, which is denoted by $\mathbb{E}(t_w)$. And $\mathbb{E}(t_w) = \mathbb{E}(t_w^1) = \mathbb{E}(t_w^2) = \dots = \mathbb{E}(t_w^J)$. From (9), the class j revenue in shared charger model is:

$$R_{e,s}^j = \theta_j \lambda \cdot (1 - P_{ro}) \cdot (R - c_w \cdot \mathbb{E}(t_w) - \mathbb{E}(c_{batt}^j) \cdot \mathbb{E}(t_{ch}^j)) \quad (13)$$

Hence, the system revenue becomes $\sum_{j \in J} R_{e,s}^j(\theta_j \lambda, SoC_r^j, S)$. Given $\theta_j, \lambda, SoC_r^j$ and S , the system revenue in shared charger model is determined.

C. TOY EXAMPLES FOR THE DEDICATED CHARGER MODEL

In our case study, enumeration method is used to determine the optimal combination of chargers $(s_1^*, s_2^*, \dots, s_J^*)$. The main procedure is as follows. First, for each value of s_j , optimal SoC_r^* method is executed to determine the optimal class revenue $R_e^j(s_j)$. Then, find the optimal combination $(s_1^*, s_2^*, \dots, s_J^*)$ by calculating $\sum_{j \in J} R_e^j$ and select the highest system revenue to be optimal.

The following case study is presented to clarify the matters. Assume there are two customer classes. Class 1 of PEVs uses DC fast charging power, with a maximum power of 45 kW. Class 2, on the other hand, prefers Level II, three-phase chargers, with a maximum power of 22 kW. The threshold energy, E_c for fast charger customers remains the same, while the threshold for the second class is determined as 5 kWh. Combined with (1), parameters in charging power model of Class 2 are $m_2 = 33$, and $n_2 = 2.2$. The system input parameters in TABLE 3 are given by $\lambda = 8$, $S = 10$, and $r_1 = r_2 = 3$. The target SoC_r is varied from 60% to 95% and the SoC_i distribution is selected as $\mathcal{N}(30, 15)$, truncated to $[5, SoC_r - 10]\%$.

TABLE 3. Toy example I – system input parameters.

Parameter	Value
total λ	8/hour
SoC_i	$\mathcal{N}(30, 15)$, truncated to $[5, SoCr-10]\%$
SoC_r	60:95%
S	10
$r_{1,2}$	3
class1	$P_{max,1}=45$ kW
class2	$P_{max,2}=22$ kW
m_2	33
n_2	2.2

We analyze the system for three population compositions, $(\theta_1, \theta_2) = \{(75\%, 25\%) (50\%, 50\%) (25\%, 75\%)\}$. The numerical results and simulation results are shown in TABLE 4 and TABLE 5, respectively. On one hand,

TABLE 4. Toy example I – numerical results.

(θ_1, θ_2)	s_j^*	SoC_r^*	Optimal system revenue (\$/hour)
(75%,25%)	(7,3)	(95%,80%)	62.31
(50%,50%)	(5,5)	(95%,85%)	60.68
(25%,75%)	(3,7)	(95%,85%)	59.63

TABLE 5. Toy example I – simulation results.

(θ_1, θ_2)	s_j^*	SoC_r^*	Optimal system revenue (\$/hour)
(75%,25%)	(7,3)	(95%,80%)	62.22
(50%,50%)	(5,5)	(95%,85%)	60.14
(25%,75%)	(3,7)	(95%,85%)	59.44

when population of one class of PEVs is relatively large, for example, class 2, the system is prone to allocate more chargers to class 2 to decrease the blocking probability and achieve higher system revenue. On the other hand, if fewer chargers are dedicated to class 2, the system is prone to decrease the SoC_r to shorten the charging time, since the average charging time of class 2 is long.

Next, we present the second toy example to evaluate the influence of different traffic loads on the dedicated

charger model. Assume SoC_r is set as 90%, and the PEV composition is selected as $(\theta_1, \theta_2)=(50\%, 50\%)$. Arrival rates of each class is varied from 1 to 7. Moreover, the total number of chargers and the waiting space for each class are chosen to be 10 and 3, respectively. The rest of the simulation parameters are given in TABLE 6.

TABLE 6. Toy example II: system input parameters.

Parameter	Value
$\lambda_{1,2}$	1:7
$SoCi$	$\mathcal{N}(30, 15)$, truncated to $[5, SoCr-10]\%$
$SoCr$	90%
S	10
$r_{1,2}$	3
class1	$P_{max,1}=45$ kW
class2	$P_{max,2}=22$ kW

For the numerical and simulation results, the optimal number of chargers for each customer class is chosen as (4, 6), and the arrival rate for each class is varied from $\lambda_j = 1 \dots 7$. The average numerical service rates for class 1 and class 2 are 2.354 and 1.151 customers/hour respectively. We further present the traffic intensity in Fig7a. The results show that simulation results support the numerical findings. It is also noteworthy that, when the arrival rate of the class 2 customers

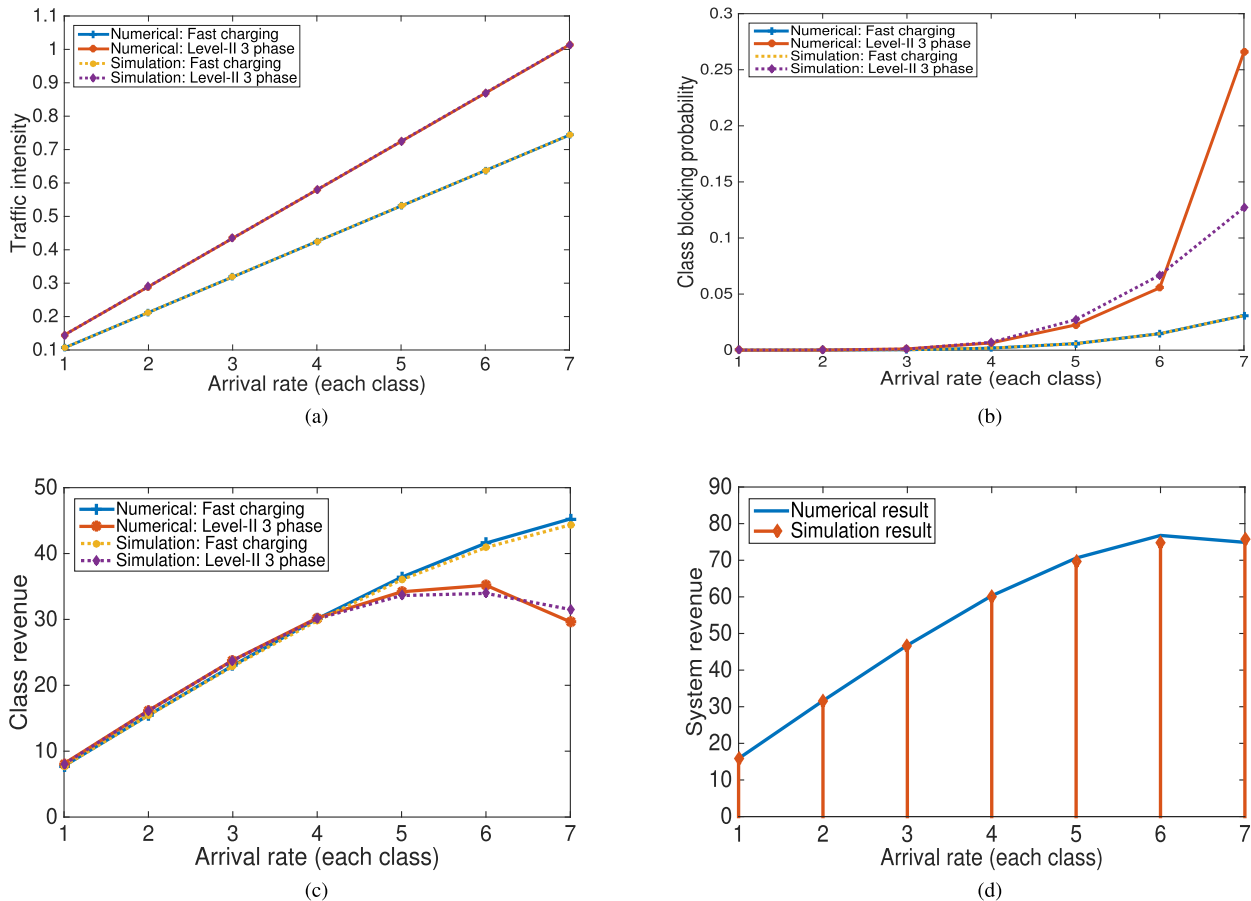


FIGURE 7. Dedicated charger model: system performance. (a) Traffic intensity: Dedicated chargers. (b) Class blocking probability Dedicated chargers. (c) Class revenue: Dedicated chargers. (d) System revenue: Dedicated chargers.

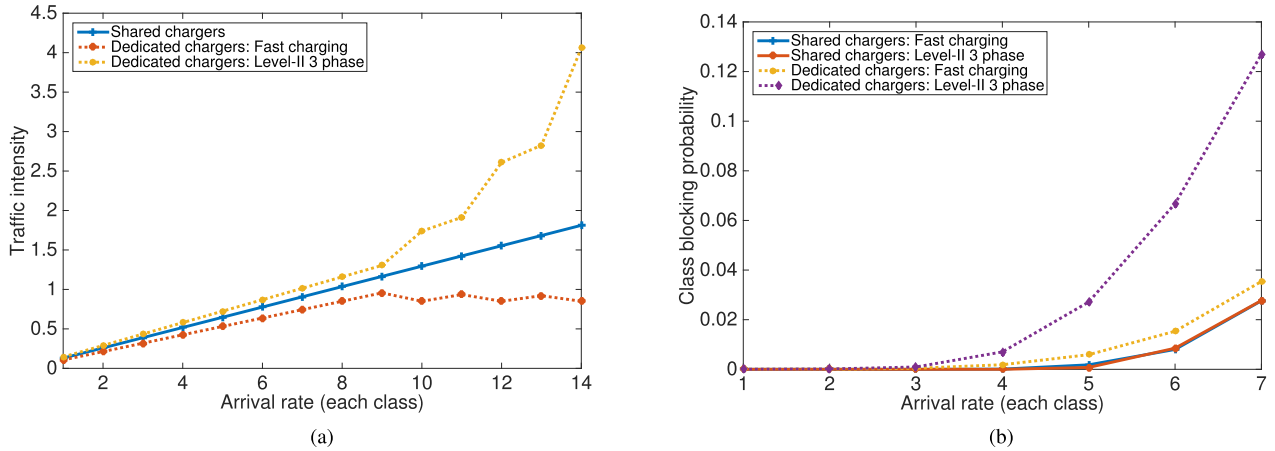


FIGURE 8. Dedicated and shared charger model: traffic intensity, blocking probability and class revenue. (a) Traffic intensity: shared and dedicated chargers. (b) Class blocking probability: shared and dedicated chargers.

approaches to $\lambda_2 = 7$, the system becomes unstable as the traffic intensity $\rho > 1$.

Moreover, we continue to present the performance metrics, Fig.7b depicts the blocking probability for each class, while Fig. 7c shows the numerical and simulation results for the revenue calculations in the multi-class setting. Fig.7d depicts the system revenue. As the arrival rate increase, operator gains higher system revenue since it can serve more customers when the blocking probability is low.

IV. PERFORMANCE ANALYSIS FOR THE MULTI-CLASS SETTING

In this section, a case study is presented to evaluate the performance of the proposed models. The main goal is to investigate the relation between the traffic intensity and resource usage. The system is simulated for 100,000 PEVs in class 1 (fast charging) and 100,000 PEVs in class 2 (level-II three phase) for both models. The system parameters are given in TABLE 6. The total waiting spaces in the shared charger model is set as $r = 6$, while in dedicated charger model the waiting spaces are $r_1 = r_2 = 3$.

In the shared charger model, the average service rate is 1.545 customers/hour. Hence, from $\rho = \frac{\lambda}{S\mu}$, the traffic density varying arrival rate from 1...14 is calculated and depicted in Fig.8a. For example, when arrival rate of each class is 5, the traffic intensity becomes $\rho = \frac{5+5}{10 \cdot 1.545} = 0.647$. In the dedicated charger model, the optimal composition of chargers allocated to each class are not equal to each other, thus, the traffic intensity varies under different traffic regimes. The results are depicted in Fig.8a. Furthermore, the mean charging time of these two classes in dedicated charger model is not the same, hence, their traffic intensities are plotted separately.

Fig.8b depicts the blocking probability of each class for the proposed models. In the shared charger model, since each PEV class share the same chargers and the waiting spaces, their blocking probabilities are the same. In dedicated charging model, the blocking probability of class 2 increases faster

than that in class 1. This is because the charging duration of class 2 is longer and this is reflected in the blocking performance. Furthermore, as the arrival rate increases, the blocking probabilities of dedicated chargers model is higher than those in shared chargers model. Hence, if the station operates under high traffic regime, system operator should choose shared charger model for better performance.

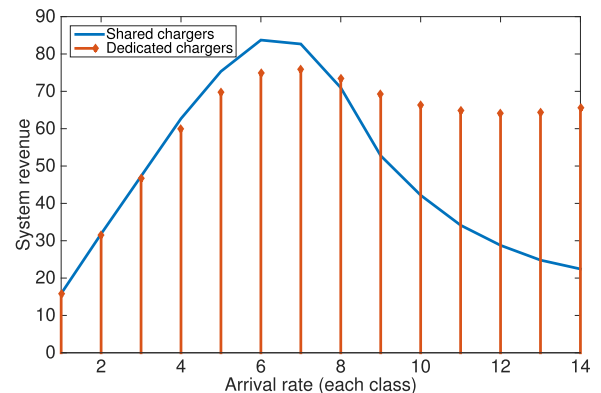


FIGURE 9. Dedicated and shared charger model: system revenue.

In Fig.9, when arrival rate of each class is low, the system revenues of two models are close. When traffic intensity becomes larger, shared charger model outperforms dedicated charger model because utilization of chargers is larger in shared charger model with increasing arrival rate. When arrival rate for each class is 6, system gains highest revenue in shared charger model. Then revenue begins to decrease in shared charger model because of heavy traffic load. From Fig.8a, when arrival rate for each class is 8, $\rho > 1$. This time, system revenue in dedicated charger model becomes larger than that in shared charger model. The reason is for the very heavy traffic load, in dedicated charger, the system allocates more chargers to fast charging class of PEVs to keep its blocking probability small. However, in shared charger model, when traffic load is very heavy, PEVs are easy to be

blocked since level-II three phase charging of PEVs occupy the chargers for long time. Hence, the blocking probability is very high and system revenue decreases dramatically.

Hence, the strategy for maximizing system revenue is that: when traffic intensity $\rho < 1$, shared charger model should be used; when $\rho \geq 1$, dedicated charger model works better.

V. CONCLUSION

In this paper, we have proposed two revenue maximization frameworks for charging station. The first framework corresponded to a revenue model for stations with single customer class. The CCCV method decreases the charging power dramatically when the battery SoC gets close to fully state, which also results in a long charging duration. Therefore, the main thrust of this work was to limit the requested SoC (SoC_r) for customers, so that more customers could be served. The system was modeled as a $M/G/S/K$ queue, where we also provided a method to generate a general charging time distributions. In this system revenue model, the PEV's cost components included battery degradation cost, the cost of waiting time, and the admission fee. Then, we determined the optimal SoC_r that maximizes the system revenue.

The second framework, on the other hand, built upon the first one and proposed a revenue model for multi-class PEVs. For this case, we proposed two different operating strategies which were shared and dedicated charger models. The system performance of each case was compared and analyzed. Our results indicated that the proposed frameworks have improved the system performance. As a future work, we will focus on the system revenue maximization in a network of charging stations.

APPENDIX

APPROXIMATION OF BLOCKING PROBABILITY AND MEAN WAITING TIME

Let $\rho = \frac{\lambda}{S\mu}$ be traffic intensity and the system is assumed to be stable and in steady state. Then the probability of having j customers in the system is [24], [25],

$$P_j = \begin{cases} \frac{(S\rho)^j}{j!} P_0 & j = 0, \dots, s-1, \\ \frac{(S\rho)^S}{S!} \frac{1-\zeta}{1-\rho} \zeta^{j-S} P_0 & j = s, \dots, K-1, \\ \frac{(S\rho)^S}{S!} \zeta^{K-S} P_0 & j = K, \end{cases} \quad (14)$$

where

$$P_0 = \left[\sum_{j=0}^{s-1} \frac{(S\rho)^j}{j!} + \frac{(S\rho)^S}{S!} \frac{1-\rho\zeta^{K-S}}{1-\rho} \right]^{-1}. \quad (15)$$

Here,

$$\zeta = \frac{\rho R_G}{1-\rho} + \rho R_G, \quad (16)$$

and

$$R_G = \frac{EW(M/G/S)}{EW(M/M/S)}, \quad (17)$$

where $EW(M/M/S)$ and $EW(M/D/S)$ are the mean waiting time in a $M/M/S$ and a $M/D/S$ systems, respectively. $EW(M/G/S)$ can be approximated in terms of $EW(M/M/S)$ and $EW(M/D/S)$ as below

$$EW(M/G/S) \approx \frac{1+c_s^2}{\frac{2c_s^2}{EW(M/M/S)} + \frac{1-c_s^2}{EW(M/D/S)}}, \quad (18)$$

where c_s^2 is the squared coefficient of variance of charging time distribution of PEVs. In terms of quantity of R_G , approximation of (17) can be rewritten as

$$R_G = \frac{(1+c_s^2)R_D}{(2R_D-1)c_s^2+1}. \quad (19)$$

where R_D is the quantity of (17) in $M/D/S$ system. $R_D = \frac{EW(M/D/S)}{EW(M/M/S)}$. Based on [25], simplified approximation of R_D is shown as follows,

$$R_D = \frac{1}{2} \left[1 + F(\theta) g(\rho) \left(1 - \exp \left\{ -\frac{\theta}{F(\theta) g(\rho)} \right\} \right) \right], \quad (20)$$

where

$$\theta = \frac{S-1}{S+1}, S \geq 1, \quad (21)$$

$$F(\theta) = \frac{\theta}{8(1+\theta)} \left(\sqrt{\frac{9+\theta}{1-\theta}} - 2 \right), \quad (22)$$

and

$$g(\rho) = \frac{1-\rho}{\rho}. \quad (23)$$

An approximation for the mean waiting time in the queue is presented next. According to Little's Law $\mathbb{E}(L_q) = \lambda \cdot \mathbb{E}(t_w)$, the value of mean waiting time $\mathbb{E}(t_w)$ can be derived if the average number of PEV in the queue $\mathbb{E}(L_q)$ is known. The method in [24] is adopted to approximate $\mathbb{E}(L_q) = \sum_{j=S}^{S+R} (j-S)P_j$ as below:

$$\mathbb{E}(L_q) = \frac{(S\rho)^S}{S!} \frac{\zeta}{(1-\rho)(1-\zeta)} \{1-\zeta^r - r(1-\zeta)\rho\zeta^{r-1}\} P_0. \quad (24)$$

Hence,

$$\mathbb{E}(t_w) = \frac{1}{\lambda} \frac{(S\rho)^S}{S!} \frac{\zeta}{(1-\rho)(1-\zeta)} \{1-\zeta^r - r(1-\zeta)\rho\zeta^{r-1}\} P_0. \quad (25)$$

REFERENCES

- [1] U.S. Government Source for Fuel Information. [Online]. Available: <http://www.fueleconomy.gov/>, accessed Oct. 2015.
- [2] (2013). *Global EV Outlook*. [Online]. Available: http://www.iea.org/publications/globalEVoutlook_2013.pdf
- [3] (2015). *Global EV Outlook*. [Online]. Available: http://www.iea.org/ev/Global-EV-Outlook-2015-Update_1page.pdf
- [4] K. Clement-Nyns, E. Haesen, and J. Driesen, "The impact of charging plug-in hybrid electric vehicles on a residential distribution grid," *IEEE Trans. Power Syst.*, vol. 25, no. 1, pp. 371-380, Feb. 2010.

- [5] A. Shortt and M. O'Malley, "Quantifying the long-term impact of electric vehicles on the generation portfolio," *IEEE Trans. Smart Grid*, vol. 5, no. 1, pp. 71–83, Jan. 2014.
- [6] S. W. Hadley, "Impact of plug-in hybrid vehicles on the electric grid," Oak Ridge Nat. Lab., Oak Ridge, TN, USA, Tech. Rep. ORNL/TM-2006/554, Oct. 2006.
- [7] I. S. Bayram, G. Michailidis, I. Papapanagiotou, and M. Devetsikiotis, "Decentralized control of electric vehicles in a network of fast charging stations," in *Proc. IEEE Global Commun. Conf.*, Atlanta, GA, USA, Dec. 2013, pp. 2785–2790.
- [8] I. S. Bayram, G. Michailidis, M. Devetsikiotis, S. Bhattacharya, A. Chakraborty, and F. Granelli, "Local energy storage sizing in plug-in hybrid electric vehicle charging stations under blocking probability constraints," in *Proc. IEEE Int. Conf. Smart Grid Commun.*, Brussels, Belgium, Oct. 2011, pp. 78–83.
- [9] P. Fan, B. Sainbayar, and S. Ren, "Operation analysis of fast charging stations with energy demand control of electric vehicles," *IEEE Trans. Smart Grid*, vol. 6, no. 4, pp. 1819–1826, Jul. 2015.
- [10] M. M. Karbasioun, I. Lambadaris, G. Shaikhet, and E. Kranakis, "Optimal charging strategies for electrical vehicles under real time pricing," in *Proc. IEEE Int. Conf. Smart Grid Commun.*, Venice, Italy, Nov. 2014, pp. 746–751.
- [11] M. Erol-Kantarci, J. H. Sarker, and H. T. Mouftah, "Quality of service in plug-in electric vehicle charging infrastructure," in *Proc. IEEE Int. Electr. Vehicle Conf.*, Greenville, SC, USA, Mar. 2012, pp. 1–5.
- [12] I. S. Bayram, G. Michailidis, M. Devetsikiotis, and F. Granelli, "Electric power allocation in a network of fast charging stations," *IEEE J. Sel. Areas Commun.*, vol. 31, no. 7, pp. 1235–1246, Jul. 2013.
- [13] I. S. Bayram, G. Michailidis, M. Devetsikiotis, and B. Parkhideh, "Strategies for competing energy storage technologies for in DC fast charging stations," in *Proc. IEEE 3rd Int. Conf. Smart Grid Commun.*, Tainan, Taiwan, Nov. 2012, pp. 1–6.
- [14] E. Yudovina and G. Michailidis, "Socially optimal charging strategies for electric vehicles," *IEEE Trans. Autom. Control*, vol. 60, no. 3, pp. 837–842, Mar. 2015.
- [15] I. S. Bayram, G. Michailidis, and M. Devetsikiotis, "Unsplittable load balancing in a network of charging stations under QoS guarantees," *IEEE Trans. Smart Grid*, vol. 6, no. 3, pp. 1292–1302, May 2015.
- [16] S. Bae and A. Kwasinski, "Spatial and temporal model of electric vehicle charging demand," *IEEE Trans. Smart Grid*, vol. 3, no. 1, pp. 394–403, Mar. 2012.
- [17] D. Ban, G. Michailidis, and M. Devetsikiotis, "Demand response control for PHEV charging stations by dynamic price adjustments," in *Proc. IEEE PES Innovative Smart Grid Technol.*, Washington, DC, USA, Jan. 2012, pp. 1–8.
- [18] A. Hoke, A. Brissette, D. Maksimović, A. Pratt, and K. Smith, "Electric vehicle charge optimization including effects of lithium-ion battery degradation," in *Proc. IEEE Vehicle Power Propuls. Conf.*, Chicago, IL, USA, Sep. 2011, pp. 1–8.
- [19] Z. Ma, S. Zou, and X. Liu, "A distributed charging coordination for large-scale plug-in electric vehicles considering battery degradation cost," *IEEE Trans. Control Syst. Technol.*, vol. 23, no. 5, pp. 2044–2052, Sep. 2015.
- [20] D. Andersson and D. Carlsson, "Measurements of ABB's prototype fast charging station for electric vehicles," M.S. thesis, Dept. Energy Environ., Division Electr. Power Eng., Chalmers Univ. Technol., Gothenburg, Sweden, 2012.
- [21] Z. Luo, Z. Hu, Y. Song, Z. Xu, and H. Lu, "Optimal coordination of plug-in electric vehicles in power grids with cost-benefit analysis—Part II: A case study in China," *IEEE Trans. Power Syst.*, vol. 28, no. 4, pp. 3556–3565, Nov. 2013.
- [22] M. Dai, J. Zheng, M. Zhang, and W. Wang, "Optimization of electric vehicle charging capacity in a parking lot for reducing peak and filling valley in power grid," in *Proc. IEEE Int. Conf. Adv. Power Syst. Autom. Protection*, vol. 2, Oct. 2011, pp. 1501–1506.
- [23] R. Hassin, Y. Y. Shaki, and U. Yovel, "Optimal service-capacity allocation in a loss system," *Naval Res. Logistics*, vol. 62, no. 2, pp. 81–97, 2015.
- [24] T. Kimura, "A transform-free approximation for the finite capacity M/G/s queue," *Oper. Res.*, vol. 44, no. 6, pp. 984–988, Nov./Dec. 1996.
- [25] T. Kimura, "Approximations for multi-server queues: System interpolations," *Queueing Syst.*, vol. 17, nos. 3–4, pp. 347–382, Sep. 1994.
- [26] N. Keon and G. Anandalingam, "A new pricing model for competitive telecommunications services using congestion discounts," *INFORMS J. Comput.*, vol. 17, no. 2, pp. 248–262, 2005.



CUIYU KONG received the B.S. degree in information engineering from the South China University of Technology, Guangzhou, China, in 2011, and the M.S. degree in communication engineering from National Central University, Taiwan, in 2013. She is currently pursuing the Ph.D. degree with the Department of Electrical and Computer Engineering, North Carolina State University, NC, USA. Her research interests are in the areas of resource allocation in networking, stochastic modeling, and control in communication and power networks.



ISLAM SAFAK BAYRAM (S'10–M'14) received the B.S. degree in electrical and electronics engineering from Dokuz Eylul University, Izmir, Turkey, in 2007, the M.S. degree in telecommunications from the University of Pittsburgh, Pittsburgh, PA, USA, in 2010, and the Ph.D. degree in computer engineering from North Carolina State University, Raleigh, NC, USA, in 2013.

He was a Post-Doctoral Research Scientist with Texas A&M University at Qatar, Doha, Qatar, in 2014. He is currently an Assistant Professor with the College of Science and Engineering, Hamad Bin Khalifa University, Doha, and a Scientist with the Qatar Environment and Energy Research Institute, Doha. His current research interests include stochastic modeling and control of communications, and power networks.

Dr. Bayram was a recipient of the best paper award at the Third IEEE International Conference on Smart Grid Communications.



MICHAEL DEVETSIKIOTIS (S'85–M'94–SM'03–F'12) was born in Thessaloniki, Greece. He received the Dipl.-Ing. degree from the Aristotle University of Thessaloniki, Greece, in 1988, and the M.Sc. and Ph.D. degrees from North Carolina (NC) State University, Raleigh, in 1990 and 1993, respectively, all in electrical engineering. In 1993, he joined the Broadband Networks Laboratory, Carleton University, Ottawa, ON, Canada, as a Post-Doctoral Fellow. He later became an Adjunct

Research Professor with the Department of Systems and Computer Engineering, Carleton University, in 1995, an Assistant Professor in 1996, and an Associate Professor in 1999. He joined the Department of Electrical and Computer Engineering, NC State University, as an Associate Professor, in 2000, and became a Professor in 2006. He is currently a member of the Eta Kappa Nu Honor Society, the Sigma Xi Honor Society, and the Phi Kappa Phi Honor Society. As a student, he received scholarships from the National Scholarship Foundation of Greece, the National Technical Chamber of Greece, and the Phi Kappa Phi Academic Achievement Award for a Doctoral Candidate at NC State University. He served as the Chairman of the IEEE Communications Society Technical Committee Communication Systems Integration and Modeling, and a member of the ComSoc Education Board. He has served as an Associate Editor of the *IEEE COMMUNICATIONS LETTERS* and an Area Editor of the *ACM Transactions on Modeling and Computer Simulation*. He has served on the Editorial Boards of the *International Journal of Simulation and Process Modeling*, the *IEEE COMMUNICATIONS SURVEYS AND TUTORIALS*, and the *Journal of Internet Engineering*. He was the Co-Chair of the Next Generation Internet Symposium under the IEEE ICC 2002, the High-Speed Networks Symposium under the IEEE ICC 2004, the Quality, Reliability and Performance Modeling (QRPM) Symposium under the IEEE ICC 2006, and the Quality, Reliability and Performance for Emerging Network Services Symposium under the IEEE Globecom 2006. He served as the Workshops Chair of the IEEE Globecom 2008, and the Co-Chair of the Workshops on Enabling the Future Service Oriented Internet (2007, 2008, and 2009). He was the Co-Chair of the QRPM Symposium under the IEEE Globecom 2010, the IEEE CAMAD 2011, Kyoto, and the QRPM Symposium at ICC 2012, Ottawa, and co-chairs tutorials of the IEEE ICC 2016. He currently serves as the Chair of GITC, the Technical Steering Committee of ICC, and Globecom.

• • •